1999

The Presence of Edge Contact and its Influence on the Debonding of Patched Panels

Anette M. Karlsson
Cleveland State University, a.karlsson@csuohio.edu

W. J. Bottega
Rutgers University - New Brunswick/Piscataway

Publisher's Statement

The final publication is available at Springer via http://dx.doi.org/10.1023/A:1018328932561

Original Citation

Karlsson, A. M., and Bottega, W. J., 1999, "The Presence of Edge Contact and its Influence on the Debonding of Patched Panels," International Journal of Fracture, 96(4) pp. 383-406.

The presence of edge contact and its influence on the debonding of patched panels

A.M. KARLSSON and W.J. BOTTEGA
Department of Mechanical and Aerospace Engineering Rutgers University Piscataway, NJ 08854-8058 U.S.A.
e-mail: bottega@rci.rutgers.edu

Abstract. A formulation is presented which accounts for configurations of debonding patched cylindrical panels for which the edge of the debonded segment of the patch maintains sliding contact with the corresponding base structure. The formulation is incorporated with that which accounts for configurations for which a contact zone is present and for which no contact between the debonded segments of the patch and base structure occurs during debonding. Analyses are performed for two types of loading conditions: Applied circumferential tension and applied internal pressure. Results of numerical simulations based on analytical solutions of the problems of interest are presented in the form of threshold and stiffness degradation curves for specific structures with various geometries, material properties and support conditions, and reveal characteristic behavior of the evolving composite structure. In particular, the effects of edge contact on the debonding scenarios of the evolving structure are elucidated.

Key words: Composite, contact, debond, delamination, doubler, edge, panel, patch, shell, structure.

1. Introduction

Multicomponent structures arranged in 'piggy back' configurations arise in a variety of applications. An example of such a composite structure is that of a repair patch adhered to a damaged base structure (see, for example, (Raizenne et al., 1995)), or a sensor adhered to a primary structure (see, for example, (Lee and Moon, 1990)). An extensive list of references pertaining to the general subject area can be found in (Bottega, 1995; Bottega and Loia, 1996, 1997) and is thus not repeated here for brevity. The issue of debonding of the secondary structure from the primary structure is clearly of interest as such behavior will evidently compromise the effectiveness and integrity of the system. Recent studies concerning edge debonding in thin structures considered both curved (Bottega and Loia, 1996) and flat (Bottega, 1995; Bottega and Loia, 1997) geometries under a variety of loading and support conditions. In those studies, an intricate array of debonding behavior was predicted, based on the mathematical model employed. The presence of a contact zone within the debonded region, as well as the situation of vanishing contact, was incorporated in the model and analysis of the evolving composite structure. A possible configuration that was not included in the prior study (Bottega and Loia, 1996) was the situation where the interior points of the debonded segments of the constituent structures are lifted away from one another while the edge of the patch maintains sliding contact with the base panel (edge contact). The incorporation of such effects into the mathematical model and their influence on the corresponding behavior of the evolving composite structure is the subject of the present study.

In this study we consider the cylindrical structures that were considered in (Bottega and Loia, 1996), but augment the model and analysis by including the possibility of edge contact.

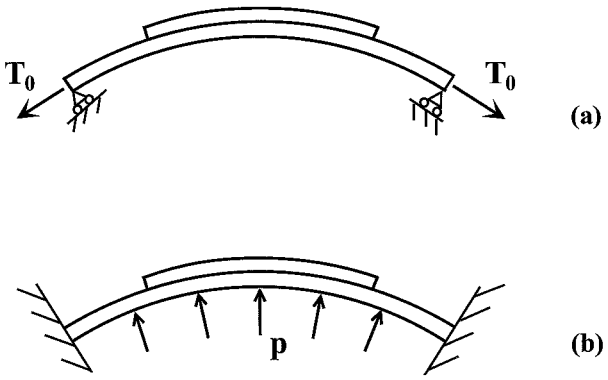

Figure 1. Patched cylindrical panel subjected to two loading types. (a) applied circumferential tension (shown with hinged-free supports). (b) applied (internal) pressure (shown with clamped-fixed supports).

In this way a direct assessment of the inclusion or omission of the effects of edge contact can be made. Two types of loading conditions are considered, as depicted in Figure 1: (1) applied circumferential tension and (2) applied (internal) pressure. (A third loading condition considered in (Bottega and Loia, 1996), three-point transverse loading, is not considered presently as such conditions are not germane to the present study.) As in the prior studies, the problems are formulated as moving interior boundary problems in the calculus of variations, with a shell theory used to model the base structure and the patch individually and a Griffith type energy criterion incorporated to govern debonding. Doing so yields a self-consistent formulation for the evolving composite structure. In what follows, the problem statement for edge contact is presented in an abbreviated form paralleling the formulation presented in (Bottega and Loia, 1996) for debonding structures with and without a continuous contact zone. Numerical simulations based on analytical solutions for edge contact, as well as for a contact zone and no contact considered in (Bottega and Loia, 1996), are then presented revealing the presence of contact and its influence on the charcteristic behavior of the evolving composite system.

2. Problem statement

In this study, we consider edge debonding of patched cylindrical panels subjected to two types of loading conditions, as shown in Figure 1. In what follows we consider configurations for which a contact zone adjacent to the bonded region may be present, configurations for which no contact of the debonded segments of the substructures occurs, and the situation where the edge of the debonded segment of the patch maintains sliding contact with the base panel during debonding (‘edge contact’). The formulation for the former two configurations is presented in (Bottega and Loia, 1996) and hence is not repeated here. It was seen therein that, within the context of the mathematical model employed, when a contact zone is present it is a ‘full’ contact zone. That is, the entire debonded segment of the patch maintains sliding contact with the base panel. We present here the formulation for the problem of edge contact of the delaminated segment of an evolving patched cylindrical panel, as a possible configuration among several, as shown in Figure 2. As the other two configurations of interest, namely ‘full contact’ and ‘no contact’, have been included in the prior study (Bottega and Loia, 1996), we consider the present case as a supplemental configuration to be incorporated into the overall analysis of the evolving composite structure, along with the others. To this end, we parallel

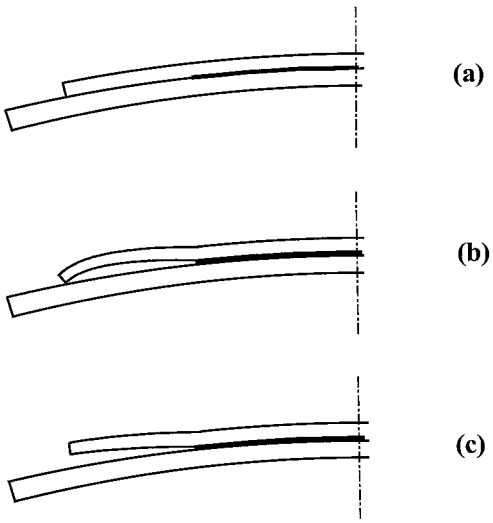

Figure 2. Deformed panel showing various configurations. (a) panel with 'full contact' of debonded segments. (b) panel with 'edge contact' of debonded segments. (c) panel with 'no contact' of debonded segments of patch and base panel.

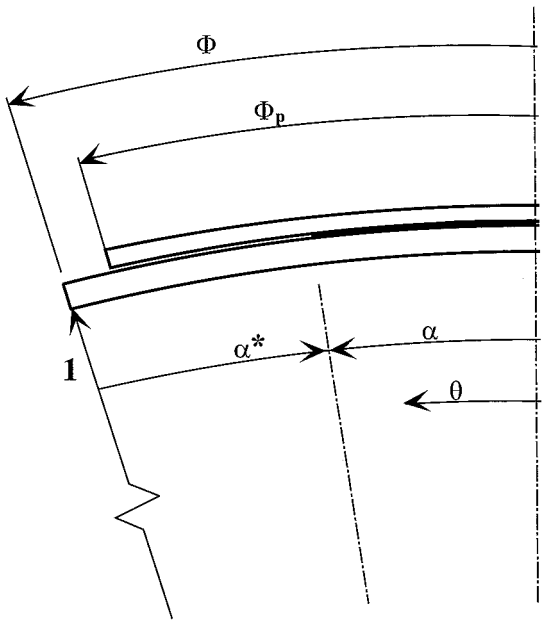

Figure 3. Half-span of panel showing characteristic lengths and coordinates.

the formulation presented in (Bottega and Loia, 1996) using the same notation and direct reference to that study where convenient.

Let us consider the half-span of a patched cylindrical panel of normalized arc length Φ to which a patch of (half) arc length Φ_p is adhered, as shown in Figure 3. As in (Bottega and Loia, 1996), all length scales are normalized with respect to the dimensional radius of the undeformed structure, throughout the presentation, and the upper surface of the base panel is used as the reference surface. The normalized circumferential coordinate θ originating

at the center of the span is therefore an angular coordinate. For the particular configuration considered presently, the patch (of normalized thickness $h_p \ll 1$) and base panel (of normalized thickness $h \ll 1$) are bonded over the region $S_1{:}\,\theta \in [0, \alpha]$ which will be referred to as the 'bond zone'. Let us also introduce the *conjugate bond zone boundary*, $\alpha^* = 1 - \alpha$, which locates the bond zone boundary with respect to the edge of the base panel. The remainder of the patch is considered to be lifted away from the base panel at all interior points defined by the region $S_2{:}\,\theta \in (\alpha, \Phi_p)$, the region of separation, but to maintain (sliding) contact with the base panel at its edge $\theta = \Phi_p$. The remaining (unpatched) segment of the base panel will be defined on the region $S_3{:}\,\theta \in (\Phi_p, \Phi]$. The base panel and the patch are modeled as independent shell segments, with the composite structure formed by the adherence of the two considered as an assemblage of these two segments. To this end, the circumferential and radial displacements, and the corresponding circumferential strain and curvature change, at the centroidal surface of the base panel within region $S_i (i = 1 - 3)$ are designated as $u_i(\theta)$ (positive away from origin) and $w_i(\theta)$ (positive inward), and $e_i(\theta)$ and $\kappa_i(\theta)$, respectively. The corresponding measures for the patch, at its centroidal surface, within region $S_i (i = 1, 2)$ are designated as $u_{pi}(\theta)$, $w_{pi}(\theta)$, $e_{pi}(\theta)$ and $\kappa_{pi}(\theta)$, in the same sense. The respective measures at the reference surface are indicated by an asterisk {i.e., $u_i^*(\theta)$, $w_i^*(\theta)$, $e_i^*(\theta)$, $\kappa_i^*(\theta)$ and $u_{pi}^*(\theta)$, $w_{pi}^*(\theta)$, $e_{pi}^*(\theta)$, $\kappa_{pi}^*(\theta)$}. The strain-displacement and curvature-displacement relations, along with the associated through the thickness variations, for the particular shell theory employed may be found in Appendix A.

As indicated in the beginning of this section, two types of loading conditions are considered. The first corresponds to the situation where the edge of the base panel is subjected to applied circumferential tension of normalized intensity T_0, and the second where the base panel is subjected to applied (internal) pressure of normalized intensity p (see Figure 1). The relation between the normalized load intensities and their dimensional counterparts may be found in Appendix C. We next introduce the constraint functional given by

$$\Lambda_2 = V_0[w_2(\Phi_p) - w_{p2}(\Phi_p)], \tag{1}$$

where $V_0 \geqslant 0$ is a Lagrange multiplier. The constraint functional defined by (1) is substituted into the energy functional defined in (Bottega and Loia, 1996), replacing the portion of the constraint functional corresponding to region S_2 defined therein (i.e., that associated with the contact zone), or equivalently, setting the parameter $\sigma_2 = 0$ in that expression.

Proceeding as in (Bottega and Loia, 1996), we arrive at a self-consistent set of constitutive relations, equilibrium equations, and boundary, matching and transversality conditions (including energy release rates) for the evolving composite structure. We thus have

$$M_1^{*\prime\prime} + M_1^* - (N_1^* w_1^{*\prime})' - N_1^* = -p, \qquad N_1^{*\prime} = 0, \quad (\theta \in S_1), \tag{2a,b}$$

$$M_2{}'' + M_2 - (N_2 w_2{}')' - N_2 = -p, \qquad N_2{}' = 0, \quad (\theta \in S_2), \tag{3a,b}$$

$$M_{p2}{}'' + M_{p2} - (N_{p2} w_{p2}{}')' - N_{p2} = 0, \qquad N_{p2}{}' = 0, \quad (\theta \in S_2), \tag{4a,b}$$

$$M_3{}'' + M_3 - (N_3 w_3{}')' - N_3 = -p, \qquad N_3{}' = 0, \quad (\theta \in S_3), \tag{5a,b}$$

with

$$w_1^*(\theta) \equiv w_1(\theta) = w_{p1}(\theta), \quad (\theta \in S_1), \tag{6a,b}$$

$$\kappa_1^*(\theta) \quad \kappa_1(\theta) = \kappa_{p1}(\theta), \quad (\theta \in S_1), \tag{6c,d}$$

$$u_1^*(\theta) = u_{p1}^*(\theta), \quad (\theta \in S_1), \tag{6e}$$

where

$$N_i(\theta) = Ce_i(\theta), \qquad M_i(\theta) = D\kappa_i(\theta) - (\tfrac{1}{2}h)N_i, \quad (i = 1 - 3) \tag{7a,b}$$

$$N_{pi}(\theta) = C_p e_{pi}(\theta), \qquad M_{pi}(\theta) = D_p \kappa_{pi}(\theta) + (\tfrac{1}{2}h_p)N_{pi}, \quad (i = 1, 2) \tag{8a,b}$$

are the normalized resultant membrane forces and bending moments in the base panel and patch, respectively, in region S_i, and

$$N_1^*(\theta) = C^* e_1^*(\theta) + B^* \kappa_1^*(\theta), \quad \text{and} \tag{9a}$$

$$M_1^*(\theta) = A^* \kappa_1^*(\theta) + B^* e_1^*(\theta) = D^* \kappa_1^*(\theta) + \rho^* N_1^*, \tag{9b}$$

respectively correspond to the normalized membrane force and normalized bending moment in the bonded portion of the composite structure. The normalized stiffnesses C, D, C_p and D_p of the primitive structures, as well as those corresponding to the intact segment of the composite structure A^*, B^*, C^*, D^* and ρ^*, are given in Appendix B. The parameter ρ^* gives the radial location of the centroid of the composite structure with respect to the reference surface. In (2)–(5), and in what follows, superposed primes indicate total differentation with respect to θ.

The associated boundary and matching conditions take the forms:

$$u_1^*(0) = 0, \qquad w_1^{*\prime}(0) = 0, \qquad [M_1^{*\prime} - N_1^* w_1^{*\prime}]_{\theta=0} = 0, \tag{10a,b,c}$$

$$u_1^*(\alpha) = u_2(\alpha) + (\tfrac{1}{2}h)w_2{}'(\alpha) = u_{p2}(\alpha) - (\tfrac{1}{2}h_p)w_{p2}{}'(\alpha), \tag{11a,b}$$

$$N_1^*(\alpha) = N_2(\alpha) + N_{p2}(\alpha), \tag{11c}$$

$$w_1^*(\alpha) = w_2(\alpha) = w_{p2}(\alpha), \qquad w_1^{*\prime}(\alpha) = w_2{}'(\alpha) = w_{p2}{}'(\alpha), \tag{11d,e,f,g}$$

$$M_1^*(\alpha) = M_2(\alpha) + M_{p2}(\alpha), \tag{11h}$$

$$[M_1^{*\prime} - N_1^* w_1^{*\prime}]_{\theta=\alpha} = [M_2{}' - N_2 w_2{}']_{\theta=\alpha} + [M_{p2}{}' - N_{p2} w_{p2}{}']_{\theta=\alpha}, \tag{11i}$$

$$u_2(\Phi_p) = u_3(\Phi_p), \qquad N_2(\Phi_p) = N_3(\Phi_p), \qquad w_2{}'(\Phi_p) = w_3{}'(\Phi_p), \tag{12a,b,c}$$

$$M_2(\Phi_p) = M_3(\Phi_p), \tag{12d}$$

$$w_{p2}(\Phi_p) = w_2(\Phi_p) = w_3(\Phi_p), \qquad N_{p2}(\Phi_p) = \kappa_{p2}(\Phi_p) = 0, \tag{13a,b,c,d}$$

$$[M_3{}' - N_3 w_3{}']_{\theta=\Phi_p} - [M_2{}' - N_2 w_2{}']_{\theta=\Phi_p} = [M_{p2}{}' - N_{p2} w_{p2}{}']_{\theta=\Phi_p} = V_0 \geqslant 0, \tag{13e}$$

$$u_3(\Phi) = 0 \quad \text{or } N_3(\Phi) = T_0 \ (T_0 \text{ prescribed}), \quad \text{and} \tag{14a,a$'$}$$

$$w_3(\Phi) = 0, \quad \text{and} \quad w_3{}'(\Phi) = 0 \text{ or } \kappa_3(\Phi) = 0. \tag{14b,c, c$'$}$$

The transversality condition for the propagating bond zone boundary α takes the form

$$\mathcal{G}^*\{\alpha\} \equiv \left[\tfrac{1}{2}D\kappa_2^2 + \tfrac{1}{2}D_p\kappa_{p2}^2 + \frac{1}{2C}N_2^2 + \frac{1}{2C_p}N_{p2}^2\right]_{\theta=\alpha} - \left[\tfrac{1}{2}D^*\kappa_1^{*2} + \frac{1}{2C^*}N_1^{*2}\right]_{\theta=\alpha} = 2\gamma, \tag{15}$$

where $\mathcal{G}^*\{\alpha\}$ is identified as the energy release rate. The condition (15) suggests the following *delamination criterion*:

if, for some initial value of $\alpha = \alpha_0$, we have that $\mathcal{G}^*\{\alpha_0\} \geqslant 2\gamma$, then debonding occurs and the system evolves (α decreases - α^* increases) such that the corresponding equality (15) *is satisfied. If $\mathcal{G}^*\{\alpha_0\} < 2\gamma$, debonding does not occur.*

Integrating (4b) and imposing condition (13c) gives

$$N_{p2}(\theta) = 0, \quad (\forall\theta \in S_2). \tag{16a}$$

Integrating (2b), (3b) and (5b) and imposing conditions (11c) and (12b), together with the result (16a), gives

$$N_1^*(\theta) = N_2(\theta) = N_3(\theta) = N_0 = \text{constant}. \quad (\forall\theta \in S_1, S_2, S_3). \tag{16b}$$

The remaining equations and conditions are modified accordingly, with the transversality condition (15) taking the form

$$\mathcal{G}^*\{\alpha\} \to \left[\tfrac{1}{2}D\kappa_2^2 + \tfrac{1}{2}D_p\kappa_{p2}^2 - \tfrac{1}{2}D^*\kappa_1^{*2} + \frac{1}{2C_e}N_0^2\right]_{\theta=\alpha} = 2\gamma, \tag{15$'$}$$

where C_e is given by (B4). Integrating the strain-displacement relations (see Appendix A) and imposing the corresponding boundary and matching conditions for the circumferential displacements results in the integrability condition given by

$$u_3(\Phi) = N_0\left[\frac{\alpha^*}{C} + \frac{\alpha}{C^*}\right] - [(h/2) + \rho^*]w'(\alpha) + \sum_{i=1}^{3}\int_{S_i}((1 - \rho^*\delta_{i1})w_i - \tfrac{1}{2}w_i'^2)\,\mathrm{d}\theta, \tag{17}$$

where δ_{ij} represents Kronecker's delta. The problem statement is thus transformed into a mixed formulation in terms of the transverse displacements $w_i(\theta)(i = 1 - 3)$, the membrane force N_0, and the propagating boundary α (or equivalently α^*).

3. Analysis

The analysis for edge contact will be conducted in a manner analogous to that performed for the same structures in (Bottega and Loia, 1996) for the configurations corresponding to a full contact zone and vanishing contact of the debonded segments of the patch and base panel. That

is, the analysis is based on the linearized version of the formulation presented in the previous section, and implemented as described below. The present results, and the regenerated results for full contact and no contact (Bottega and Loia, 1996), will then be incorporated to establish augmented scenarios of the evolving structure. We first outline the method of analysis for edge contact configurations.

3.1. EQUILIBRIUM PATHS

To determine the critical equilibrium paths corresponding to configurations for which edge contact is present, we follow the same general procedure established in (Bottega and Loia, 1996) and (Bottega, 1995) for configurations for which a contact zone was present or for which no contact of the debonded segments of the evolving structure occurs. Thus, we first define the normalized loading parameter λ and characteristic deflection Δ for each of the specific loading types presently under consideration. We thus have, for the cases of applied circumferential tension and applied (internal) pressure respectively,

$$\{\lambda = T_0,\ \Delta = \Delta_c \quad u_3(\Phi)\} \quad \text{and} \quad \{\lambda = p,\ \Delta = \Delta_0 \ \equiv -w_1(0)\}. \tag{18a,b}$$

We likewise define the 'global stiffness' for each particular problem as

$$K \quad \lambda/\Delta, \tag{19}$$

for each (λ, Δ) pair defined in (18).

Since the analysis to be performed is a linear one, and hence the response in each case will be proportional to the loading parameter for the specific problem under consideration, the intergrability condition, represented by (17), will take the general form

$$u_3(\Phi) = \lambda \mathcal{F}_\lambda(\alpha) + N_0 \mathcal{F}_N(\alpha), \tag{20}$$

where $\mathcal{F}_\lambda(\alpha)$ and $\mathcal{F}_N(\alpha)$ are functions obtained by substituting the specific analytical solution for the transverse displacement into (17). For problems of applied circumferential tension $\lambda = T_0$, we have from boundary condition (14a′) that $N_0 = T_0$. Equation (20) then gives the normalized circumferential edge displacement as a function of the applied tension for this case. For the case of applied pressure, (20) gives the normalized membrane force N_0 as a function of p for fixed end conditions $[u_3(\Phi) = 0]$, and gives the circumferential edge displacement as a function of the applied pressure p for free edge conditions, where $N_0 = 0$ from (14a′).

With the above established, the energy release rates for the case of edge contact can be expressed in terms of the loading parameter explicitly, for each case under consideration. The equations for the growth paths/threshold curves λ vs. α (or α^*) and Δ vs. α (or α^*) may then be found directly from the transversality condition (15′), and take the general forms

$$\lambda^* \quad \lambda/\sqrt{2\gamma} = 1/\sqrt{\Omega(\alpha; \mathbf{S})}, \qquad \Delta^* \quad \Delta/\sqrt{2\gamma} = K^{-1}(\alpha; \mathbf{S})/\sqrt{\Omega(\alpha; \mathbf{S})}, \tag{21a,b}$$

where $\Omega(\alpha; \mathbf{S})$ is the normalized energy release rate per square of the normalized load, $\mathbf{S}$ is the set of stiffnesses of the structure, and (λ^*, Δ^*) correspond one to one with each (λ, Δ) pair defined previously. Corresponding paths pertaining to alternative configurations are regenerated as in (Bottega and Loia, 1996), and incorporated as needed.

3.2. EVOLVING STRUCTURES

The threshold curves generated as described above correspond to configurations of edge contact (configurations for which all interior points of the debonded segments of the patch and base panel are lifted away from one another, while the edge of the patch maintains sliding contact). Other possible configurations include those for which no contact of the debonded segments occur, and those for which a contact zone is present adjacent to the bond zone boundary. These later two types of equilibrium configuration were included in the study presented in (Bottega and Loia, 1996). It was shown therein that, within the context of the mathematical model employed, a contact zone will not exist for the case of tensile loading regardless of the support conditions at the edge of the structure. It was, however, seen that a contact zone can and often does exist for the case of pressure loading when the edges of the base panel are clamped so as to prohibit rotation (whether free or fixed with regard to circumferential translation). It was demonstrated that when a contact zone does exist, for the structures and loading types considered, that it is a full contact zone. That is that every point of the debonded segment of the patch maintains sliding contact with the base panel, and hence that the situation of an intermediate or propagating contact zone such as occurs in certain delamination problems (see for example (Bottega, 1994)) is not an issue for the present class of problems. We are here interested in the incorporation of results concerning configurations associated with the presence of edge contact, together with the results of the previous study (Bottega and Loia, 1996), so as to present an augmented study of the debonding of patched panels. To this end, a hierarchy of admissible equilibrium configurations must be established for a given loading type, for situations in which two or more of the configurations discussed (full contact, edge contact, no contact) are admissible (physically realizable solutions can be found) for a given structure and support conditions for a specific value of the conjugate bond zone size. In this regard, the 'preferred' configuration will be identified as that for which the system possesses the lowest total energy per unit load, as characterized by the work per unit intensity of the applied load, $\mathcal{W}^*$. Thus, for $T_0 = 1$ or $p = 1$, we respectively have

$$\mathcal{W}^* = u_3(1) \quad \text{or} \quad \mathcal{W}^* = -\sum_{i=1}^{3} \left\{ \int_{S_i} w_i \, \mathrm{d}\theta \right\} \tag{22a,b}$$

which may be evaluated by direct substitution of the corresponding analytical solution into (17) or (22b) as appropriate. In this way, the augmented characterization of the evolution of the debonding structure may be performed using the analytical solution for each particular problem of interest. Results pertaining to the specific structures examined in (Bottega and Loia, 1996) are presented in the next section.

4. Results and discussion

Results are presented for the two loading types under consideration: (i) applied circumferential tension and (ii) applied (internal) pressure. For each case, the threshold curves/equilibrium paths corresponding to edge contact are generated and then incorporated with the results presented in (Bottega and Loia, 1996) pertaining to a full contact zone and to vanishing contact, providing an augmented interpretation of the scenarios discussed therein. As in (Bottega and Loia, 1996), we consider the specific base structure of half-span $\Phi = 0.4$ and normalized thickness $h = 0.02$, to which a patch of equal thickness is adhered ($h_p = h$). The effect of

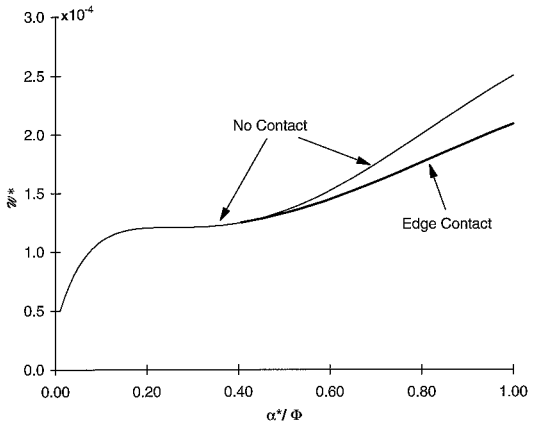

Figure 4. Work per unit load for edge contact and no contact configurations, for representative structure ($E_0 = 1$, $\Phi_p/\Phi = 1$) subjected to applied (cirumferential) tension.

relative stiffness of the patch and base structure is examined by considering several modulus ratios, E_0, as defined by (B2). Specifically, we consider the modulus ratios $E_0 = 0.1$, 1.0, and 10.0, throughout. The effect of the relative length of the patch is examined as well. In each case, the effect of the support conditions on the behavior of the evolving structure is examined by considering various combinations of fixing and freeing the edges of the base panel with regard to rotation and circumferential translation. It was shown in (Bottega and Loia, 1996) that a contact zone does not exist when the edges of the structure are free to rotate (i.e., the case of pinned supports). It is likewise found presently that edge contact does not occur either for this type of support condition. (Contact is generally associated with the presence and location of an inflection point or pseudo inflection point along the span of the deformed structure.) The scenarios for both tensile and pressure loading for structures with pinned supports thus remain as discussed in (Bottega and Loia, 1996). This is not so for the case where the edges of the base panel are clamped so as to prohibit rotation. We first consider the case of applied circumferential tension.

4.1. Applied circumferential tension

We first consider the situation where the composite structure is subjected to circumferentially directed tensile loading of normalized intensity T_0 applied at the edges of the base panel, as shown in Figure 1a. The edges are considered to be free to translate circumferentially, but clamped so as to prohibit rotation (clamped-free supports). It was shown in (Bottega and Loia, 1996) that a contact zone does not exist for this type of loading condition. However, in addition to the configurations for which no contact of the debonded segments of the patch and base panel takes place (Bottega and Loia, 1996), it is found presently that configurations for which edge contact occurs are possible as well. As discussed in Section 3.2, in situations where two or more configurations are admissible for a given conjugate bond zone size α^*, the 'preferred' configuration will be taken to be the one for which the total energy of the system per unit load is the lowest for a particular patch and base structure, where the total energy is characterized by the work per unit load $\mathcal{W}^*$. As an example, let us consider the work per unit load for the case of a structure where the patch is of the same length and modulus of the base structure ($\Phi_p = \Phi$, $E_0 = 1$), shown in Figure 4. It may be seen from the figure that

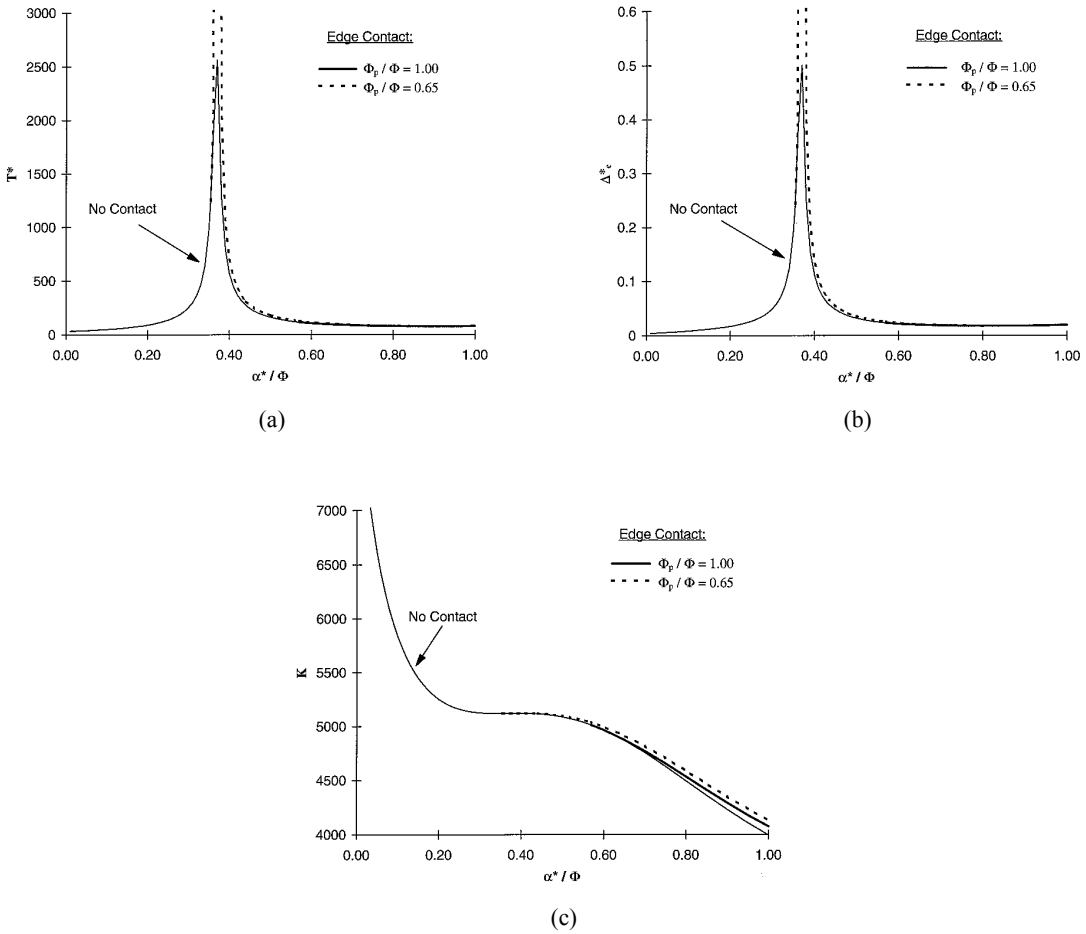

Figure 5. Threshold curves for patched panel, with clamped supports, subjected to applied (circumferential) tension for the case of $E_0 = 0.1$, for selected relative patch lengths: (a) renormed tension vs conjugate bond zone size, (b) renormed circumferential edge deflection vs conjugate bond zone size, (c) global stiffness vs conjugate bond zone size.

edge contact configurations are possible for conjugate bond zone sizes which are larger than about 40 percent of the span for this case. It is also seen that when admissible solutions corresponding to edge contact configurations exist, the associated work per unit load is consistently below that of the configuration for no contact, and hence that edge contact is the 'preferred configuration' in this case. Similar results are found for all cases considered. That is that edge contact configurations are 'preferred' over no contact configurations. The corresponding figures are omitted for brevity. In what follows, results are sequentially presented for modulus ratios $E_0 = 0.1$, 1.0, and 10.0, for various relative lengths of the patch.

$E_0 = 0.1$

Threshold and stiffness degradation curves for various patch lengths are displayed in Figures 5a,b,c–6a,b,c for relatively compliant patches ($E_0 = 0.1$). In each, the equilibrium path corresponding to configurations of no contact (NC) are displayed with the associated paths corresponding to configurations of edge contact (EC), the latter being dependent on the

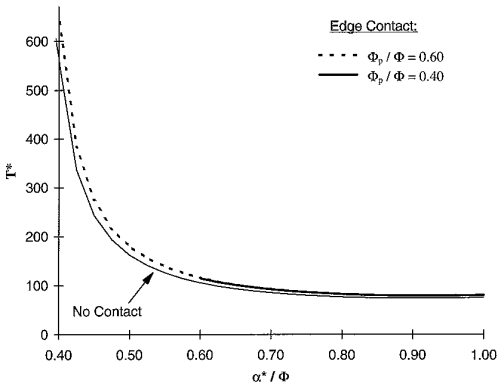

(a–i)

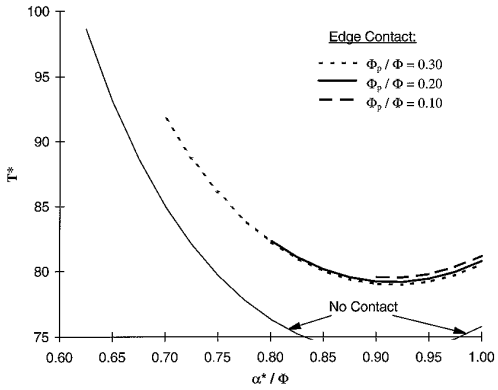

(a–ii)

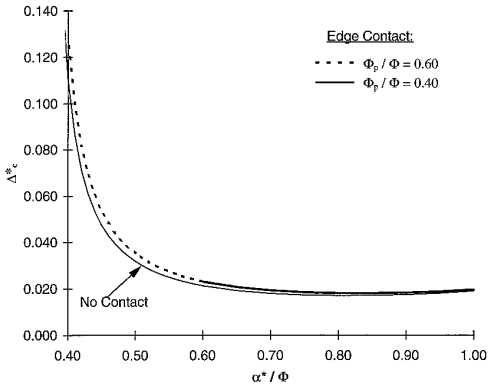

(b–i)

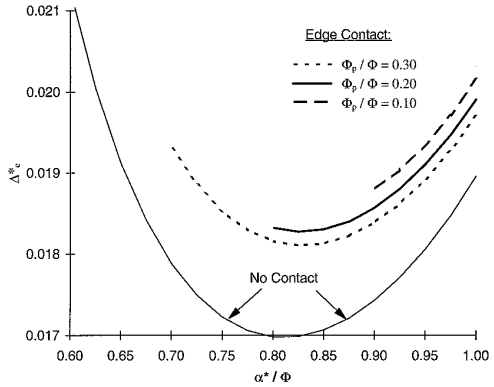

(b–ii)

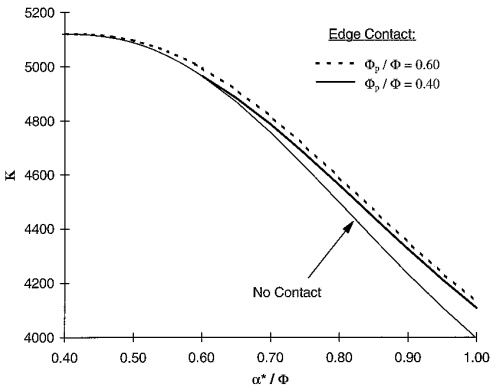

(c–i)

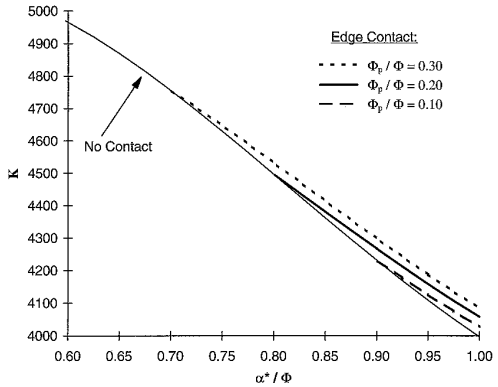

(c–ii)

Figure 6. Threshold curves for patched panel, with clamped supports, subjected to applied (circumferential) tension for the case of $E_0 = 0.1$, for selected relative patch lengths: (a–i,ii) renormed tension vs conjugate bond zone size, (b–i,ii) renormed circumferential edge deflection vs conjugate bond zone size, (c–i,ii) global stiffness vs conjugate bond zone size.

total length of the patch, Φ_p. Specifically, Figures 5a and 6a display the threshold curves/ delamination paths expressed in terms of the renormed tension T^* as a function of the conjugate bond zone size α^*, Figures 5b and 6b show the threshold curves expressed in terms of the renormed circumferential edge deflection Δ_c^*, and Figures 5c and 6c display the associated stiffness degradation curves. The EC paths associated with the patch lengths within the range considered in Figures 5a–c are seen to initiate at progressively smaller values of $\alpha^* > \Phi - \Phi_p$ as the patch length is diminished, while the EC paths associated with patch lengths within the range $0 < \Phi_p/\Phi \leqslant 0.6$, shown in Figures 6a–c, are seen to be admissible for the entire range of physically realizable values of $\alpha^*(\Phi - \Phi_p \leqslant \alpha^* < \Phi)$. Thus, debonding of patches which are of moderate to small relative lengths is seen to always be accompanied by edge contact. Let us consider each range more closely. Consideration of Figure 5a shows that, for force controlled loading, a patch which is of the same total length as the base panel and is initially bonded over most of its length (α_0^* to the left of the peak of the NC path) will initially debond in a stable manner and with no contact once the indicated level of the applied tension is achieved. The figure indicates that stable debonding will continue, with incremental increases in the applied tension accompanied by progressively smaller incremental increases in the debonded area, until the corresponding peak level is achieved ($T^* \approx 2600$) at which point unstable and catastrophic debonding ensues at constant tension, with edge contact being initiated at $\alpha^*/\Phi \approx 0.57$ and maintained throughout the subsequent unstable debonding. For the same patch length, but for initial conjugate bond zone sizes to the right of the peak, the paths indicate that debonding will always be unstable and catastrophic once the critical tension level is achieved, progressing first without contact and then with edge contact. Debonding of patches of this length, with large enough initial debonded area, will catastrophically debond with edge contact throughout the debonding process. Fully bonded patches of length $\Phi_p/\Phi = 0.65$ are seen to initially debond in a stable manner, first without contact but with edge contact initiating almost immediately. Stable debonding is seen to continue, as the applied tension is increased, until the tension level associated with the peak of the corresponding edge contact path is achieved, $T^* \approx 35,000$ (not seen within the scale of the figure) at which point unstable and catastrophic debonding ensues. Patches of this length ($\Phi_p/\Phi = 0.65$), but with initial conjugate bond zone sizes to the right of the peak of the EC path, will debond catastrophically once the corresponding critical tension is achieved. In both situations, debonding progresses in the presence of edge contact. It is seen that, for this case, the threshold levels corresponding to the 'preferred' edge contact configuration are higher, and the stable debonding less rapid (more stable), than would be predicted if edge contact were neglected. The paths displayed in Figure 5b indicate that corresponding behavior, for deflection controlled loading is similar, the exception being that patches with large enough initial debonded areas will debond in a (rapidly) stable manner when the critical deflection is achieved, for patch lengths within the range indicated. Consideration of Figures 6a–i and 6a–ii indicates that shorter patches, those of total length $\Phi_p/\Phi \leqslant 0.6$, debond in an unstable and catastrophic manner once debonding ensues and, as mentioned earlier, do so with the presence of edge contact. It is seen that the threshold levels indicated by the EC paths are higher than those which would be predicted if the presence of edge contact was neglected. It may be seen from Figure 6a–ii that very short patches, as well as patches of any length with very small initial bond areas, debond in an unstable followed by a stable manner or in a (rapidly) stable manner depending on the initial bond zone size. (This last subtle characteristic was not seen within the resolution of Figures 5a and 6a–i, nor for the NC path within the resolution of the corresponding figure in (Bottega and Loia, 1996)).

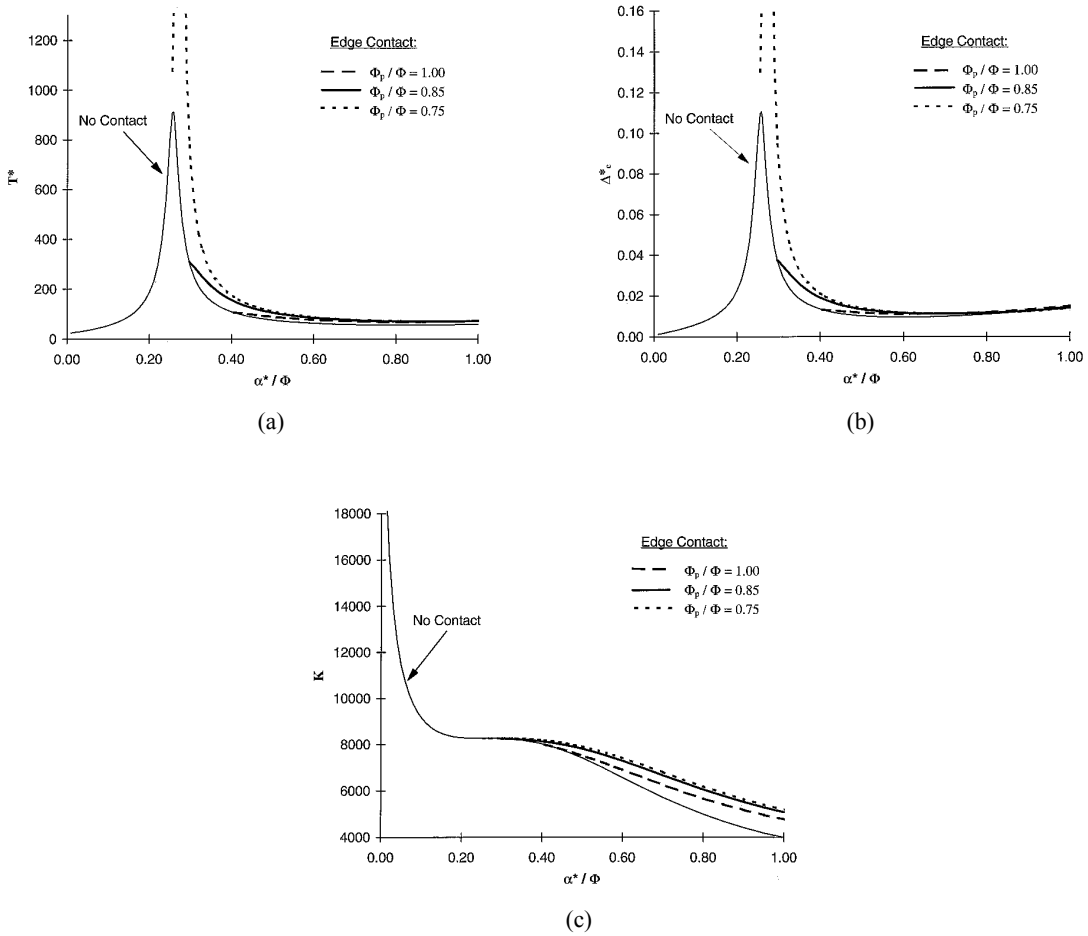

Figure 7. Threshold curves for patched panel, with clamped supports, subjected to applied (circumferential) tension for the case of $E_0 = 1.0$, for selected relative patch lengths: (a) renormed tension vs conjugate bond zone size, (b) renormed circumferential edge deflection vs conjugate bond zone size, (c) global stiffness vs conjugate bond zone size.

$E_0 = 1.0$

The threshold and stiffness degradation curves corresponding to patches of intermediate relative modulus, $E_0 = 1.0$, are displayed in Figures 7a,b,c–8a,b,c for various relative patch lengths. Comparison of these figures with those previously discussed for the case of compliant patches, indicates that the onset of edge contact ('touch down') occurs at smaller values of the conjugate bond zone size for the stiffer structures. Edge contact is seen to initiate at progressively larger conjugate bond zone sizes ($\alpha^* > \Phi - \Phi_p$) as the total length of the patch diminishes, for the relatively long patches with lengths in the range 0.75 Φ_p/Φ 1.0. Edge contact is seen to occur for all physically realizable $\alpha^*(\Phi - \Phi_p$ $\alpha^* < \Phi)$ for shorter patches. Consideration of the individual paths for specific patch lengths offers debonding scenarios analogous to those discussed for the compliant patches, with stable debonding followed by catastrophic debonding or unstable and catastrophic debonding, etc., progressing with or without edge contact as indicated.

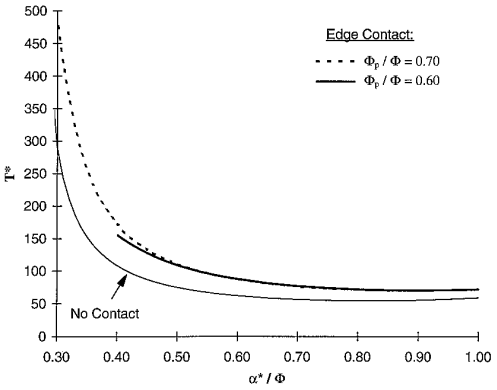

(a–i)

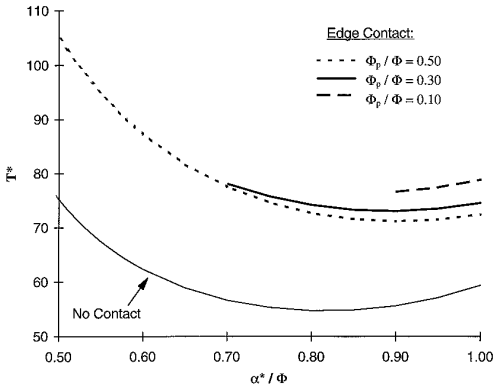

(a–ii)

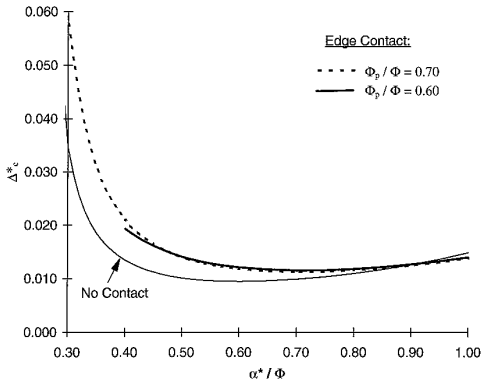

(b–i)

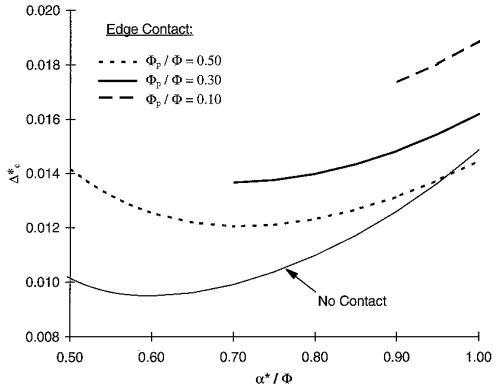

(b–ii)

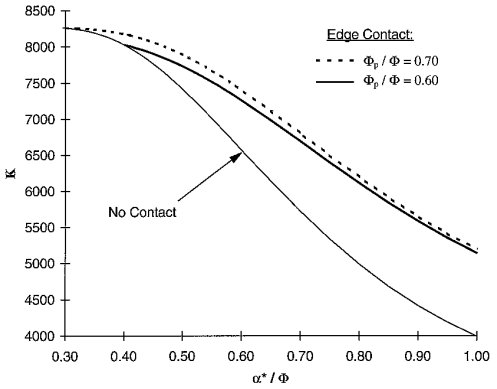

(c–i)

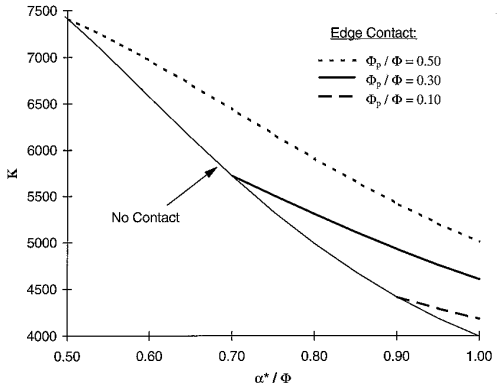

(c–ii)

Figure 8. Threshold curves for patched panel, with clamped supports, subjected to applied (circumferential) tension for the case of $E_0 = 1.0$, for selected relative patch lengths: (a–i,ii) renormed tension vs conjugate bond zone size, (b–i,ii) renormed circumferential edge deflection vs conjugate bond zone size, (c–i,ii) global stiffness vs conjugate bond zone size.

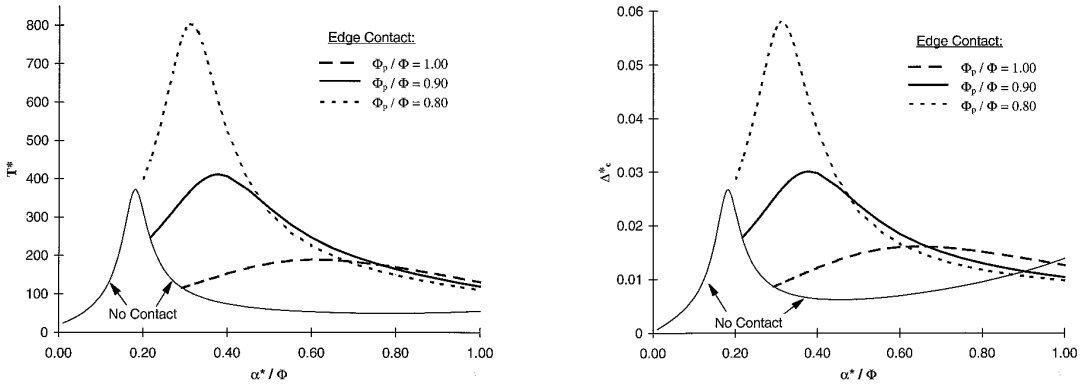

(a) (b)

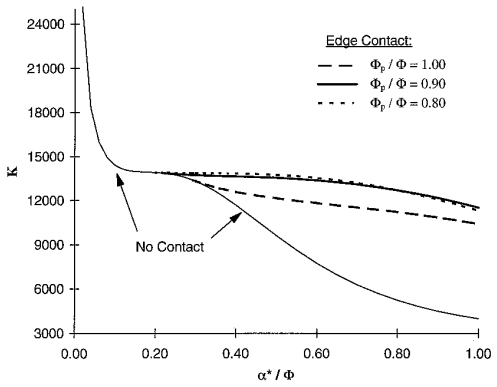

(c)

Figure 9. Threshold curves for patched panel, with clamped supports, subjected to applied (circumferential) tension for the case of $E_0 = 10.0$, for selected relative patch lengths: (a) renormed tension vs conjugate bond zone size, (b) renormed circumferential edge deflection vs conjugate bond zone size, (c) global stiffness vs conjugate bond zone size.

$E_0 = 10$

For this last case, threshold and stiffness degradation curves corresponding to relatively stiff patches, $E_0 = 10$, are displayed in Figures 9a,b,c–10a,b,c. The paths corresponding to edge contact configurations are seen to significantly deviate from those corresponding to configurations of no contact. Hence, the inclusion of edge contact is seen to substantially alter the predicted behavior of the debonding structure for this case. Consideration of these figures shows that edge contact initiates at progressively smaller conjugate bond zone sizes ($\alpha^* > \Phi - \Phi_p$) as the patch length diminishes, for patches with total length within the range 0.8 Φ_p/Φ 1.0, while edge contact is seen to occur for all physically realizable $\alpha^*(\Phi - \Phi_p$ $\alpha^* < \Phi)$ for the shorter patches considered (Φ_p/Φ 0.7). The debonding behaviors of stiff patches are seen to exhibit a variety of characteristics as follows. We first consider the relatively long patches of Figures 9a–c. The behavior of the full length patch ($\Phi_p/\Phi = 1.0$) may be implied from the corresponding paths in Figure 9a. For a patch with an initial conjugate bond zone size to the left of the peak of the NC path, debonding will

initiate when the critical tension level indicated by the NC path is achieved, with debonding progressing in a stable manner until the peak level is achieved (T^* 370). At this point unstable debonding ensues, with 'touch down' occuring at α^*/Φ 0.29 and edge contact being maintained while unstable and catastrophic debonding progresses. For initial bond zone sizes $\alpha_0^*/\Phi \geqslant 0.29$, debonding begins when the tension level indicated by the EC path is achieved. Once this occurs, debonding progresses in a stable followed by an unstable and catastrophic manner, or in a catastrophic manner, depending upon the initial value of α^*. For a patch whose length is 90 percent that of the base panel, initial debonding of fully bonded, or almost fully bonded, patches progresses in a stable manner with no contact until the peak of the NC path is achieved. At this point unstable debonding ensues, at constant T^*, with edge contact initiating where indicated and debond growth progressing until the EC path is intercepted (α^*/Φ 0.32). Debonding with edge contact then progresses in a stable manner until the peak in the corresponding EC path is achieved, after which it progresses in an unstable and catastrophic manner. For patches of the same length but with $\alpha_0^*/\Phi \geqslant 0.22$, debonding will ensue when the critical level indicated by the corresponding EC path is achieved and will progress in a stable followed by an unstable and catastrophic manner, or in a catastrophic manner, depending on the initial conjugate bond zone size. The debonding scenarios for structures with patches of relative length $\Phi_p/\Phi = 0.8$ are similar, however a small region of arrest following a small amount of unstable debonding occurs once the peak level of the NC path is achieved is indicated for this case. Scenarios for deflection controlled loading of patches with lengths in the range just discussed are similar. Debonding scenarios for shorter patches, Φ_p/Φ 0.7, may be assessed upon consideration of Figures 10a–10c. As discussed earlier, we first note that edge contact is present for all physically realizable values of α^* for this range of patch lengths. Upon consideration of Figure 10a it may seen that, for force controlled loading, patches which are initially fully bonded, or almost fully bonded (α^*/Φ 1–Φ_p/Φ), will first debond in a stable manner once the critical tension level indicated by the associated EC curve is achieved. After a very small amount of (rapid) stable debonding, debonding progresses in an unstable and catastrophic manner when the applied tension reaches the level indicated by the corresponding peak. Structures possessing a slightly greater amount of initial debonding (i.e., those with an initial conjugate bond zone size to the right of the corresponding peak) will debond catastrophically once the critical tension is achieved. Consideration of Figure 10b shows similar behavior for deflection controlled loading, with the exception that the range of values of α^* for which stable debonding is indicated is significantly larger to the extent that for the shortest patches considered (Φ_p/Φ 0.4) only stable debonding is indicated.

4.2. Applied (internal) pressure

We next consider the case where the composite structure is subjected to radially directed pressure of normalized intensity p, as indicated in Figure 1b. Two types of support conditions will be considered: (i) *clamped-free*, where the edges of the base panel are clamped so as to prohibit rotation and free so as to allow circumferential translation, and (ii) *clamped-fixed*, where the supports prohibit both rotation and circumferential translation of the edges of the base panel. It was seen in (Bottega and Loia, 1996) that structures with clamped supports (free or fixed), that are subjected to transverse pressure, admit configurations corresponding to a full contact zone (FCZ) as well as to no contact (NC) of the debonded segments. It will be seen that such structures also admit configurations corresponding to edge contact (EC) of the debonded segments of the patch and base panel. However, unlike for the case of applied

circumferential tension loading, while giving a more correct depiction of the physical events pertaining to the genesis of the evolving composite structure, the influence of edge contact with regard to the critical load levels and stability of the debonding process is found to be minimal, particularly for the case of clamped-fixed supports. In each case, we incorporate the results pertaining to edge contact together with the prior results of (Bottega and Loia, 1996) pertaining to full contact and no contact. We first consider the case of clamped-free support conditions.

Clamped-Free Supports

Figure 11 depicts the work per unit pressure for the representative case corresponding to a patch of modulus ratio $E_0 = 1.0$ and relative length $\Phi_p/\Phi = 1.0$. Based on the discussion presented in Section 3.2, it is seen from Figure 11 that the hierarchy of admissible configurations is (1) full contact, (2) edge contact and (3) no contact. Such results are typical, hence corresponding results for other cases considered are not presented for brevity.

Threshold curves corresponding to structures with a patch of relative length $\Phi_p/\Phi = 0.9$ and modulus ratios $E_0 = 0.1$, $E_0 = 1.0$ and $E_0 = 10$ are displayed in Figures 12a, 12b and 12c respectively. In each case, the paths corresponding to each possible configuration, where admissible and expressed in terms of the renormed pressure p^* as a function of the conjugate bond zone size α^*, are displayed. Paths corresponding to structures with a patch of modulus ratio $E_0 = 1.0$ are displayed for relative patch lengths $\Phi_p/\Phi = 1.0, 0.9$ and 0.8 in Figures 13a, 13b and 13c, respectively. We recall from (Bottega and Loia, 1996) that patches with lengths $\Phi_p/\Phi < 0.78$ do not admit contact for this case. Consideration of Figures 12a–c shows the full contact path and the unstable branch of the no contact path to be separated by an asymptote. (As in (Bottega and Loia, 1996) the NC path possesses a stable branch to the left of the asymptote that is not shown since it is never achieved – i.e., it corresponds to the least preferred configuration.) The path corresponding to edge contact configurations, for the range of values of α^* for which they are the 'preferred' configuration, is also shown in the figure. It is seen that the debonding scenario for cases in which the initial conjugate bond zone size α_0^* lies to the left of the corresponding asymptote is not altered by the presence of edge contact. In these situations debonding is seen to progress in a stable manner, with a full contact zone, and to effectively arrest as α^* approaches the asymptote. The debonding scenarios for cases in which the initial conjugate bond zone size lies slightly to the right of the asymptote are, however, altered. For such situations, debonding is seen to ensue, with edge contact, once the critical pressure level indicated by the EC path is achieved. Debonding with edge contact is seen to progress in an unstable manner (mildly stable for $E_0 = 10$) for the short range of conjugate bond zone sizes indicated, with the patch then lifting away from the base panel ('lift off'). Debonding then progresses in an unstable and catastrophic manner with no contact of the debonded segments occurring. It may be seen that the indicated threshold levels within this range of α^* can be significantly lower than would be predicted if edge contact were not taken into account. Debonding scenarios for patches with larger initial conjugate bond zone sizes (out of the indicated range of the EC path and to its right) are unaltered from previously predicted (see (Bottega and Loia, 1996)).

Clamped-Fixed Supports

The work per unit pressure for the representative case of a patch of modulus $E_0 = 0.1$ and of the same length as the base panel ($\Phi_p/\Phi = 1$), is shown in Figure 14. The hierarchy of admissible configurations is seen to be the same as for the case of clamped-free supports.

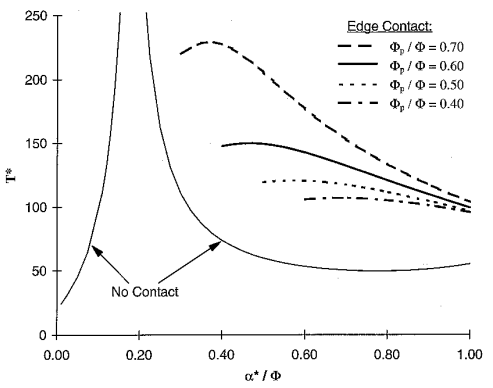

(a–i)

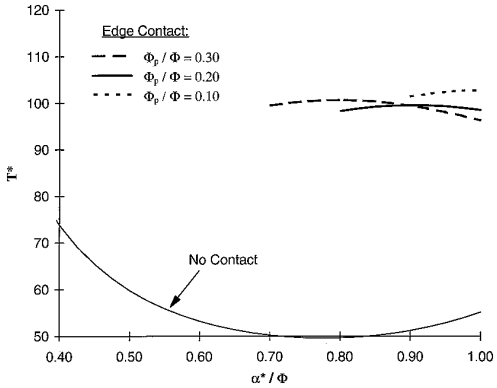

(a–ii)

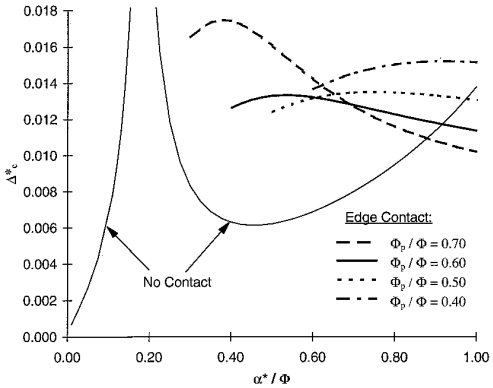

(b–i)

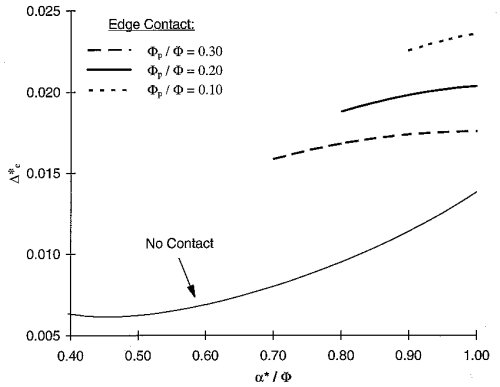

(b–ii)

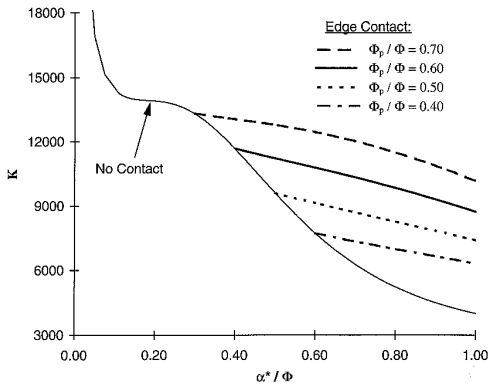

(c–i)

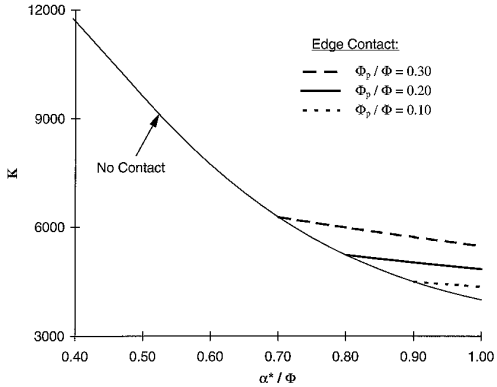

(c–ii)

Figure 10. Threshold curves for patched panel, with clamped supports, subjected to applied (circumferential) tension for the case of $E_0 = 10.0$, for selected relative patch lengths: (a–i,ii) renormed tension vs conjugate bond zone size, (b–i,ii) renormed circumferential edge deflection vs conjugate bond zone size, (c–i,ii) global stiffness vs conjugate bond zone size.

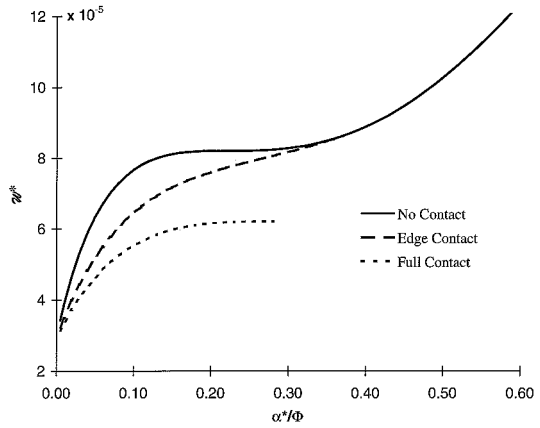

Figure 11. Work per unit load for full contact, edge contact and no contact configurations, for representative structure ($E_0 = 1$, $\Phi_p/\Phi = 1$) with *clamped-free supports*, subjected to applied (internal) pressure.

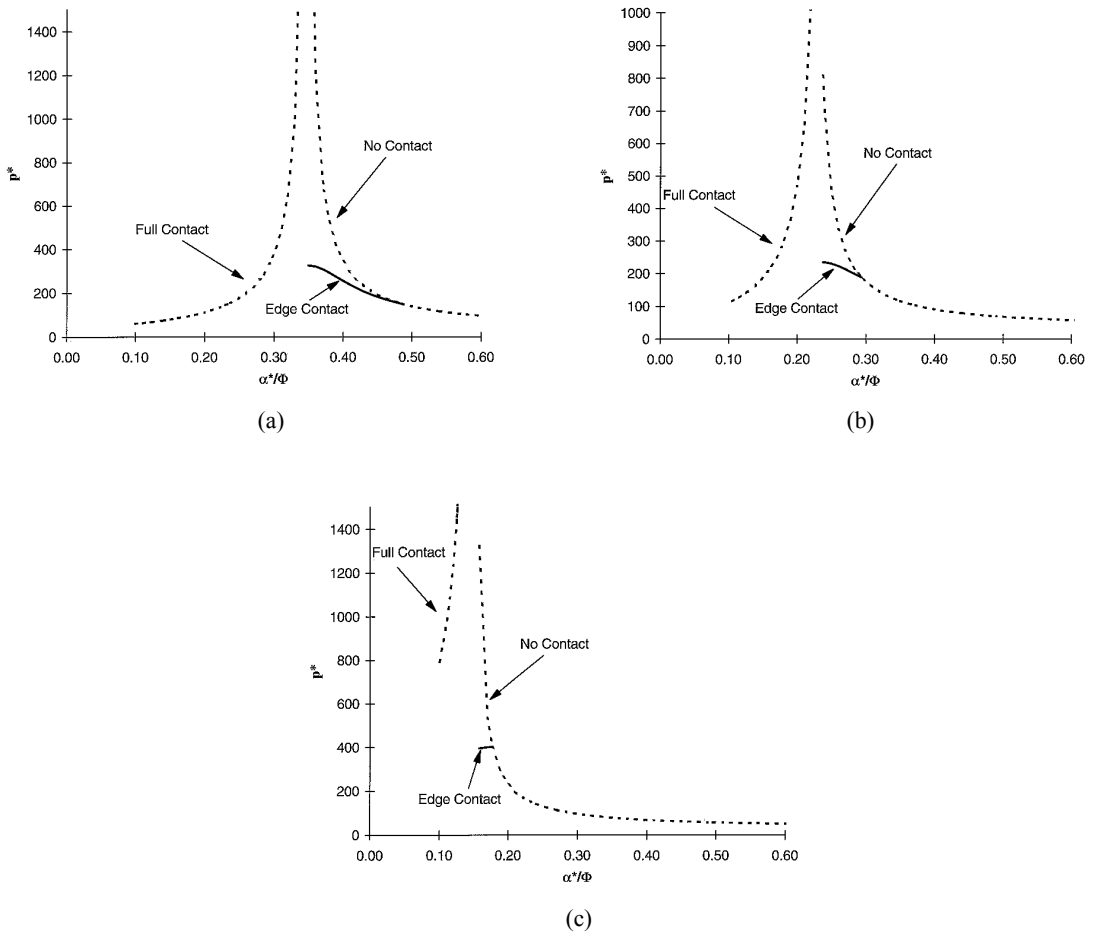

Figure 12. Threshold curves for patched panel, with *clamped-free supports*, subjected to applied (internal) pressure for the case $\Phi_p/\Phi = 0.9$: (a) $E_0 = 0.1$, (b) $E_0 = 1.0$, (c) $E_0 = 10.0$.

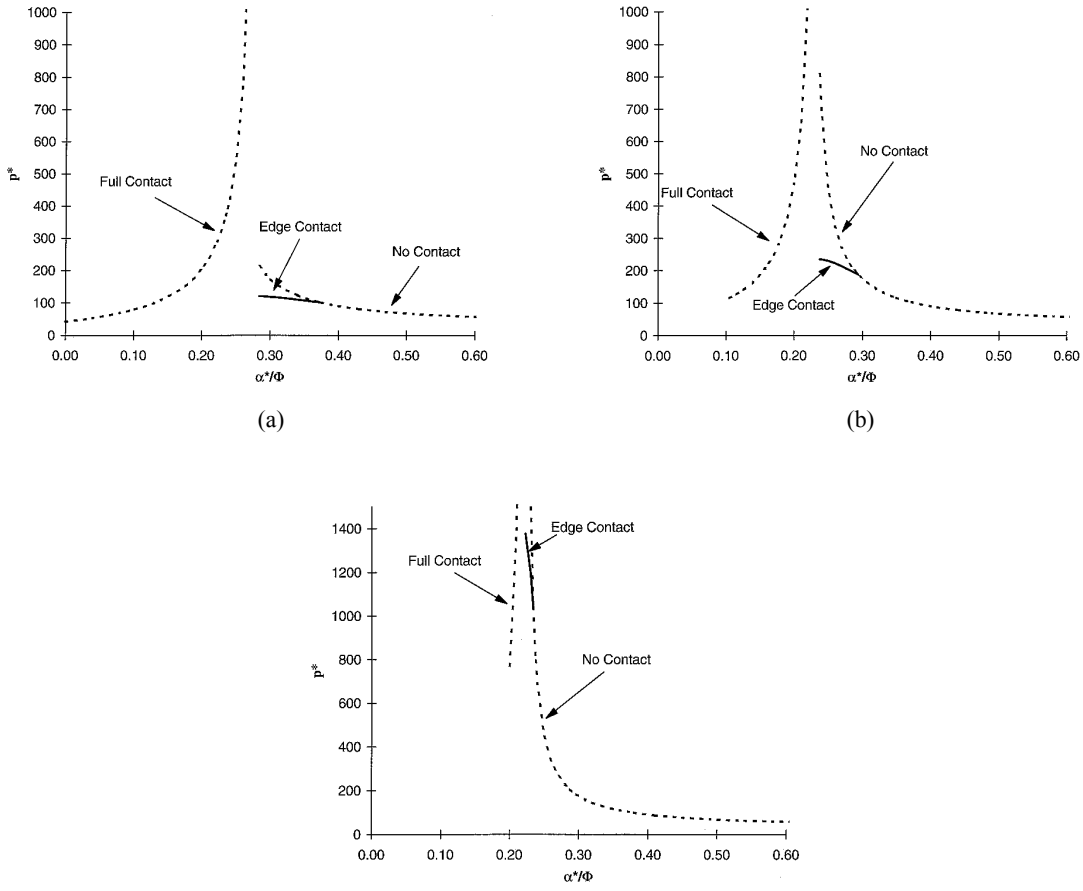

Figure 13. Threshold curves for patched panel, with *clamped-free supports*, subjected to applied (internal) pressure for the case $E_0 = 1.0$: (a) $\Phi_p/\Phi = 1.0$, (b) $\Phi_p/\Phi = 0.9$, (c) $\Phi_p/\Phi = 0.8$.

That is, the order of preference of the system is (1) full contact, (2) edge contact, (3) no contact. Similar results are found for all structures considered, but are omitted for brevity. The corresponding threshold curves, expressed in terms of the renormed pressure p^*, are displayed in Figure 15. In that figure, the portion of the EC path within the range of values for which edge contact is the preferred configuration (effective range of EC) is darkened so as to emphasize its influence. Upon consideration of Figure 15, it is seen that the debonding scenario is unchanged for initial conjugate bond zone sizes to the left of the asymptote of the full contact zone path. That is that debonding ensues once the corresponding threshold value indicated on the FCZ curve is achieved, for structures possessing initial values of α^* within this range, and debonding progresses in a stable manner with a full contact zone and effectively arrests as the asymptote is approached. For structures possessing initial values of α^* to the right of the asymptote, within the range of values for which a full contact zone is admissible, debonding will ensue once the corresponding threshold level indicated on the FCZ curve is achieved and will progress in an unstable manner with a full contact zone to the point where the FCZ path ceases and the effective range (darkened portion) of the EC path begins. At this point the interior points of the debonded segment of the patch lift away from the

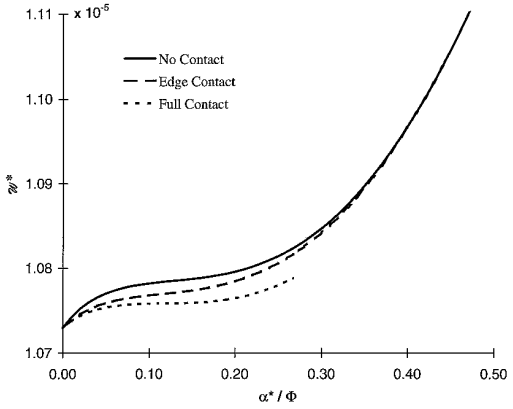

Figure 14. Work per unit load for full contact, edge contact and no contact configurations, for representative structure ($E_0 = 0.1, \Phi_p/\Phi = 1.0$) with *clamped-fixed* supports, subjected to applied (internal) pressure.

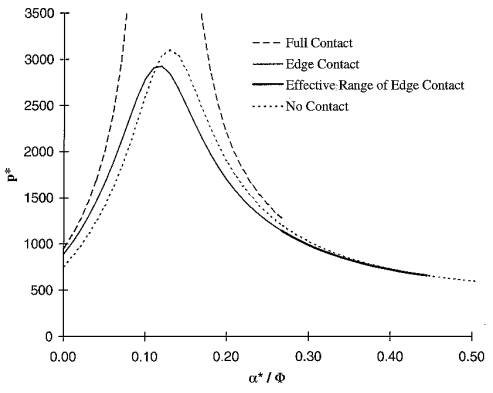

Figure 15. Threshold curves for representative patched panel ($E_0 = 0.1, \Phi_p/\Phi = 1.0$) with *clamped-fixed supports*, subjected to applied (internal) pressure.

Table 1. Path coordinates corresponding to the perimeters of the *effective range of edge contact* for selected patched panels under applied (internal) pressure, for the case of *clamped-fixed supports*.

Parameters		Start of edge contact		End of edge contact	
E_0	Φ_p/Φ	α^*/Φ	p^*	α^*/Φ	p^*
1.0	1.0	0.116	638	0.165	504
0.1	1.0	0.267	1140	0.445	657
0.1	0.9	0.260	1220	0.365	802
0.1	0.8	0.258	1270	0.294	1050

base panel and unstable debonding progresses, in the presence of edge contact, until the point where the EC path ceases. At this point the edge of the patch lifts away from the base panel, as well, and unstable and catastrophic debonding progresses with no contact. Structures with larger initial debonded regions corresponding to initial values of α^* out of the range of the EC path debond without contact of the debonded segments as described in the previous study (Bottega and Loia, 1996). It is thus seen that, within its effective range, the EC curve is almost coincident with the NC curve. Thus, while the sequence of full contact to edge contact to no contact during unstable debonding, within the range of conjugate bond zone sizes indicated, is more thoroughly captured with the inclusion of edge contact, the difference in threshold level and the degree of stabilty is affected in a very minor way when compared with results which neglect the effects of edge contact. Similar effects of edge contact are seen for the remaining structures considered in (Bottega and Loia, 1996) for the case of clamped-fixed supports. These results are presented in an abbreviated form, with the corresponding range of values of α^* and threshold pressures at the end points of the effective range for edge contact listed in Table 1. The values listed in the table can be 'superposed' on the corresponding figures

presented in (Bottega and Loia, 1996) for direct evaluation of the effects of edge contact for those cases. Similar results are also seen for deflection controlled loading, upon examination of the corresponding Δ_0^* vs α^* paths, but these paths and corresponding data are not shown for brevity.

5. Concluding remarks

The existence and effects of edge contact configurations, those for which the edge of the debonded segment of the patch maintains sliding contact with the base panel, on the debonding of patched cylindrical panels has been examined. The formulation for such problems was presented and numerical simulations based on analytical solutions were performed. The corresponding results, expressed in the form of threshold curves, were incorporated together with regenerated results of prior studies (Bottega and Loia, 1996) in which configurations for which a contact zone was present or no contact of the debonded segments of the patch and base structure occured. Two types of loading conditions were studied. These include applied circumferential tension and applied (internal) pressure. Edge contact was found for both loading types when the edges of the base panel were constrained from rotating (i.e., clamped), but not when the edges were free to rotate (i.e., pinned). For the case of tension loading, edge contact was found to occur often, particularly for moderate to short patch lengths. For such patch lengths edge contact was always present during debonding. In contrast, long patches were seen to develop edge contact only after a certain amount of debonding without contact occurred. The amount of precontact debonding was seen to increase with the patch length. For such loading and support conditions, the corresponding debonding scenarios were seen to be altered, often substantially, from those which would be predicted if the presence of edge contact was not included in the analysis. For these cases, however, the influence of edge contact was generally in the conservative sense, usually raising the threshold levels and often stabilizing debond growth. For the case of pressure loading with clamped supports (free or fixed), edge contact did not occur for moderate to short patches but was found to occur for a small range of debond sizes for relatively long patches. For these structures, circumstances for which (stable or unstable) debonding with a contact zone was previously predicted (Bottega and Loia, 1996) were seen to be unaltered. Situations where unstable debonding without a contact zone was previously predicted, where a large enough initial debond was present, were now often found to occur with edge contact for a limited range of intermediate bond zone sizes. Thus, a sequence of configurations of full contact to edge contact to no contact during unstable debonding was seen for relatively long patches. The corresponding threshold pressures, in these cases were observed to be slightly lower than would be predicted if edge contact were not taken into account. In general, however, the inclusion of edge contact was not generally seen to effectively alter the debonding scenarios for the case of pressure loading. Finally, we remark that parallel studies concerning the flat patched structures considered in (Bottega, 1995) did not show the presence of edge contact for the particular geometries, moduli and patch lengths considered therein, regardless of support conditions. To close, it was seen that edge contact can and often does occur, and its presence can influence the debonding behavior of structures of the type considered.

Appendix A: Deformation-displacement relations

Strain-displacement and curvature-displacement relations for centroidal surfaces of base panel and patch, respectively:

$$e_i = u_i' - w_i + \tfrac{1}{2}w_i'^2, \qquad \kappa_i = w_i'' + w_i, \quad \theta \in S_i \quad (i = 1, 2, 3), \tag{A1a,b}$$

$$e_{pi} = u_{pi}' - w_{pi} + \tfrac{1}{2}w_{pi}'^2, \qquad \kappa_{pi} = w_{pi}'' + w_{pi}. \quad \theta \in S_{ip} \quad (i = 1, 2), \tag{A1c,d}$$

Circumferential displacements and membrane strains at reference surface:

$$u_i^* = u_i + (\tfrac{1}{2}h)w_i', \qquad e_i^* = e_i + (\tfrac{1}{2}h)\kappa_i, \quad (i = 1, 2, 3), \tag{A2a,b}$$

$$u_{pi}^* = u_{pi} - (\tfrac{1}{2}h_p)w_{pi}', \qquad e_{pi}^* = e_{pi} - (\tfrac{1}{2}h_p)\kappa_{pi}, \quad (i = 1, 2). \tag{A2c,d}$$

Appendix B: Stiffnesses

Normalized membrane and bending stiffnesses of base panel and patch

$$C = 12/h^2, \qquad D = 1, \qquad C_p = CE_0h_0, \qquad D_p = E_0h_0^3, \tag{B1a–d}$$

where

$$h_0 = h_p/h, \tag{B1e}$$

and E_0 is given by (B2).

Modulus ratio of patch to base panel

$$E_0 = E_p/E \quad \text{or} \quad E_0 = \frac{E_p/(1-\nu_p^2)}{E/(1-\nu^2)}, \tag{B2a,b}$$

where E and E_p correspond to the (dimensional) elastic moduli of the base panel and patch, respectively, and ν and ν_p correspond to the associated Poisson's ratios.

Normalized Stiffnesses of intact segment of the composite structure:

$$A^* = D + D_p + (h/2)^2C + (h_p/2)^2C_p, \qquad B^* = (h_p/2)C_p - (h/2)C, \tag{B3a,b}$$

$$C^* = C + C_p, \qquad D^* = A^* - \rho^*B^* = D + D_p + (h^*/2)^2C_s, \tag{B3c,d}$$

where

$$\rho^* = B^*/C^*, \quad h^* = h + h_p \ll 1 \quad \text{and} \quad C_s = CC_p/C^*. \tag{B3e,f,g}$$

'Jump' in membrane stiffness /'equivalent stiffness' at bond zone boundary

$$1/C_e = \frac{(C_p/C)}{C^*}. \tag{B4}$$

Appendix C: Normalization of loads and bond energy

The normalized loads and bond energy are related to their dimensional counterparts as

$$T_0 = \overline{T}\,\overline{R}^2/\overline{D}, \qquad p = \overline{p}\overline{R}^3/\overline{D}, \qquad \gamma = \overline{\gamma}\overline{R}^2/\overline{D}, \tag{C1–C3}$$

where $\overline{T}$, $\overline{p}$ and $\overline{\gamma}$, are the dimensional tension, pressure and bond energy, respectively, $\overline{D}$ is the dimensional bending stiffness of the base panel and $\overline{R}$ is the dimensional radius of the undeformed structure. The normalized contact force, V_0 (the Lagrange multiplier), is related to its dimensional counterpart in the same manner as the applied tension.

Acknowledgement

The authors wish to thank D.W. Oplinger of the Federal Aviation Administration for his support and encouragement. This work was supported by the FAA through the Rutgers University Center for Computational Modeling of Aircraft Structures (CMAS).

References

Bottega, W.J. (1994). On circumferential splitting of a laminated cylindrical shell. *International Journal of Solids and Structures* **31**, 1891–1909.

Bottega, W.J. (1995). Separation failure in a class of bonded plates. *Composite Structures* **30**, 253–269.

Bottega, W.J. and Loia, M.A (1996). Edge debonding in patched cylindrical panels. *International Journal of Solids and Structures* **33**, 3755–3777.

Bottega, W.J. and Loia, M.A. (1997). Axisymmetric edge debonding in patched plates. *International Journal of Solids and Structures* **34**, 2255–2289.

Lee, C.K. and Moon, F.C. (1990). Modal sensors/actuators. *ASME Journal of Applied Mechanics* **57**, 434–441.

Raizenne, M.D., Heath, J.B.R. and Gaudertt, P.C. (1995). Failure analysis of bonded boron doublers. *Proceedings of the National Research Council of Canada Symposium on Composite Repair of Aircraft Structures*, University of British Columbia, Vancouver, Aug. 9–10, pp. 10.1–10.30.